NOTICE

CERTAIN DATA CONTAINED IN THIS DOCUMENT MAY BE DIFFICULT TO READ IN MICROFICHE PRODUCTS.

LA-UR 91-2911

LA-UR--91-2911

DE92 000258

Los Alamos National Laboratory is operated by the University of California for the United States Department of Energy under contract W-7405-ENG-36.

Received by OSTI

OCT 0 4 1991

TITLE: CYGNUS COLLABORATION CONTRIBUTIONS TO THE TWENTY-SECOND ICRC

AUTHOR(S): *D. E. Alexandreas, D. Berley, S. Biller, R. L. Burman, D. R. Cady, C. Y. Chang, B. L. Dingus, C. L. Dion, G. M. Dion, R. W. Ellsworth, S. J. Freedman, B. K. Fujikawa, J. A. Goodman, T. J. Haines, C. M. Hoffman, D. A. Krakauer, P. W. Kwok, X-Q Lu, D. E. Nagle, M. E. Potter, V. D. Sandberg, C. Sinnis, M. J. Stark, T. Tsutsumi, D. Williams, D. D. Weeks, G. B. Yodh, and W. P. Zhang*

SUBMITTED TO: Proceedings of the 22nd ICRC Conference, Dublin, Ireland, August 12-23, 1991

DISCLAIMER

This report was prepared as an account of work sponsored by an agency of the United States Government. Neither the United States Government nor any agency thereof, nor any of their employees, makes any warranty, express or implied, or assumes any legal liability or responsibility for the accuracy, completeness, or usefulness of any information, apparatus, product, or process disclosed, or represents that its use would not infringe privately owned rights. Reference herein to any specific commercial product, process, or service by trade name, trademark, manufacturer, or otherwise does not necessarily constitute or imply its endorsement, recommendation, or favoring by the United States Government or any agency thereof. The views and opinions of authors expressed herein do not necessarily state or reflect those of the United States Government or any agency thereof.

By acceptance of this article, the publisher recognizes that the U.S. Government retains a nonexclusive, royalty-free license to publish or reproduce the published form of this contribution, or to allow others to do so, for U.S. Government purposes.

The Los Alamos National Laboratory requests that the publisher identify this article as work performed under the auspices of the U.S. Department of Energy.

LosAlamos Los Alamos National Laboratory
Los Alamos,New Mexico 87545

FORM NO. 836 R4
ST. NO. 2629 5/81

DISTRIBUTION OF THIS DOCUMENT IS UNLIMITED

MASTER

August, 1991

Cygnus

CYGNUS Collaboration Contributions to the 22nd ICRC

Dublin, Ireland

Search for Daily Emission of Ultra High Energy Air Showers from Point Sources with the CYGNUS Experiment

The CYGNUS Collaboration

D.E. Alexandreas,[1] D. Berley,[2] S. Biller,[1] R.L. Burman,[3] D.R. Cady,[4] C.Y. Chang,[2] B.L. Dingus,[2] C. Dion,[2] G.M. Dion,[1] R.W. Ellsworth,[5] S.J. Freedman,[6] B.K. Fujikawa,[6] J.A. Goodman,[2] T.J. Haines,[2] C.M. Hoffman,[3] D.A. Krakauer,[6] P.W. Kwok,[2] X-Q Lu,[1] D.E. Nagle,[3] M. Potter,[3] V.D. Sandberg,[3] C. Sinnis,[3] M.J. Stark,[2] T. Tsutsumi,[7] D. Williams,[2] D.D. Weeks,[7] G.B. Yodh,[1] and W.P. Zhang,[3]

[1] *The University of California, Irvine*
[2] *The University of Maryland, College Park*
[3] *Los Alamos National Laboratory, Los Alamos, New Mexico*
[4] *The University of Notre Dame, Notre Dame, Indiana*
[5] *George Mason University, Fairfax, Virginia*
[6] *Argonne National Laboratory, Argonne, Illinois*
[7] *University of New Mexico, Albuquerque, New Mexico*

presented by Gaurang B. Yodh

Abstract

The CYGNUS extensive air shower experiment has been operating continuously since April, 1986. We have searched the entire data set for daily excesses of ultra high energy extensive air showers from the directions of 44 possible point astrophysical sources. These sources include Cyg X-3, Her X-1, the Crab, a number of X-ray sources from the COS-B and the fourth Uhuru catalogs, several cataclysmic variables, nearby galaxies and pulsars. The observed daily excesses are consistent with expectations based on statistical fluctuations of the background cosmic rays, although a few potentially interesting days are described.

INTRODUCTION: The CYGNUS extensive air shower experiment, located at 106.3° W and 35.9°N, has been continuously operating since April, 1986, and has been continuously expanded. As of May, 1990, it has a total number of 204 scintillation counters, covering an area of 85,000 m^2. It has a nominal energy threshold of 40 TeV and an angular resolution of 0.75°[1], which dictates a bin size of 2.4° × 2.4°/$cos\delta$ to search for point sources. A total number of 210 million air shower events have been recorded to date. A search for long term emissions from various potential point sources have been reported elsewhere[2]. We have found no evidence for steady emission from these sources. It is, however, possible that

Table 1: List of all the potential sources searched and their right ascensions and declinations (1950.0 epoch).

Source	$\alpha(°)$	$\delta(°)$	Source	$\alpha(°)$	$\delta(°)$	Source	$\alpha(°)$	$\delta(°)$
Cyg X-3	307.7	40.8	PSR1957+20	299.4	22.7	U Gem	118.0	22.1
Her X-1	254.0	35.4	4U0115+63	18.8	63.5	AM Herc	273.7	49.8
Crab	82.9	22.0	4U0042+32	10.5	32.8	SS Cygni	325.2	43.3
2CG095+04	318.9	55.0	4U0316+41	49.1	41.3	HZ 43	198.5	29.4
Geminga	97.4	17.8	4U0352+30	58.1	30.9	DQ Her	271.5	45.9
2CG078+01	305.4	39.8	4U1918+15	289.7	15.0	1E2259+58	344.8	58.6
2CG075+00	304.8	36.4	4U1954+31	298.5	32.0	V404 Cygni	300.4	33.8
2CG065+00	298.7	28.7	4U1956+35	299.1	35.1	Virgo A	186.9	12.7
2CG135+01	38.2	61.7	4U2142+38	325.6	38.1	Andromeda	9.9	41.0
2CG121+04	7.2	66.5	4U2321+58	350.3	58.6	K1	36.0	32.3
PSR1953+29	298.3	29.3	4U1257+28	194.4	28.2	K3	270.3	42.6
PSR1937+21	294.4	21.5	4U1651+39	252.9	39.9	K4	36.2	61.1
PSR1929+10	292.5	10.9	4U1957+40	299.3	40.5	K5	352.7	67.4
PSR0355+54	58.8	54.1	4U2358+21	359.7	21.1	K6	3.4	25.9
PSR1951+32	197.8	32.7	GK Per	52.0	43.7			

the emission of UHE gamma rays is episodic in nature. The length of such bursts could vary from minutes to days. In this paper we report the results of a search for daily emissions from a list of 44 potential point sources for the period of April 1986 through July 1991. The negative results reported by this search, of course, do not exclude the existence of bursts of very different durations.

SEARCH METHOD: The data is segmented into sources days for each source. Each source day consists of 24 sidereal hours centered at the source transit time. The number of events from a particular source over a particular day is compared with the expected number of events. The expected number of events for each source on each day is estimated using a randomization method. The essence of this method is as follows. Each air shower event can be characterized by (θ_i, ϕ_i, t_i) in the local horizontal coordinates, where θ_i is the zenith angle, ϕ_i the azimuthal angle, and t_i the time when the event occurred. The local coordinates are transformed into the equatorial coordinates (α, δ) for all events and those that fall within a source bin are counted as on-source events. In the local coordinates, a fake event is generated by randomly associating the (θ_i, ϕ_i) of an event with the time, t_j, of another event. The local coordinates of these fake events are transformed into equatorial coordinates (α, δ) and those that fall within a source bin are counted as off-source events. For each real event, ten fake events are generated so that the off-source estimates have ten times of the statistics of the on-source observations. This method is equivalent to a right ascension scan with five bins on either side of the source bin. The advantages of this method are that it naturally takes into account the variations of (θ, ϕ) distributions in the local

coordinates and the trigger rate variations with time due to local air pressure changes.

SEARCH RESULTS: We have applied the method described above to the entire CYGNUS data set. The sources we have looked at are listed in Table 1. Among those are Cyg X-3, Her X-1, and Crab which are the three most studied objects in our energy regime. In addition, the list includes 7 COS-B sources[3], 6 radio pulsars, 13 *Uhuru* X-ray sources[4], 6 classic cataclysmic variables, and a few other interesting objects. We have also looked at the five spots in the sky (K1, K3, K4, K5, and K6) which had the largest excesses in the air shower data collected by the University of Kiel group[5].

The results from this search are presented in Figure 1, which is the distribution of the daily excess in terms of standard deviations (number of sigmas) from all sources calculated according to the prescription of Li-Ma[6]. Superimposed on the histogram is a properly normalized gaussian distribution with mean equal to zero and a unit standard deviation. From this figure we conclude that we have not observed any statistically significant daily excesses from any of the 44 sources with our data set covering calendar time from April 1986 to July 1991. To facilitate communications with other groups, the six days with the largest excesses in Figure 1 are listed with their UT date in Table 2.

We have noticed a recent report[7] by the SOUDAN-II group of excesses of underground muons from the direction of Cyg X-3 during the January 1991 radio outbursts. We have looked our data and found no excesses of air showers from Cyg X-3 over the same period of time.

Using the fact that we observe roughly 100 events from a source in the course of a transit (the exact number depends on the declination of the source), an nominal energy threshold of 40 TeV, and a cosmic ray flux of $f_{CR}(E > 40TeV) = 2.9 \times 10^{-11} cm^{-2} \cdot sec^{-1}$ in the angular bin used in this search, we arrive at a typical daily upper limit on the gamma rays flux from a source of $f_\gamma(> 40TeV) < 3.6 \times 10^{-12} cm^{-2} \cdot sec^{-1}$.

ACKNOWLEDGEMENTS: We would like to thank R.S. Delay for his continued assistance in maintaining and operating the experiment. We would also like to thank R. Barrone, M. Gilra, and E. Horch for their assistance with data processing. Many of us would like to thank the MP Division of Los Alamos National Laboratory for their hospitality. This work is supported in part by the National Science Foundation, Los Alamos National Laboratory, the U.S. Department of Energy, and the Institute of Geophysics and Planetary Physics of the University of California.

References

[1] D. E. Alexandreas *et al.*, Phys. Rev. D43 1735 (1991).

[2] D. E. Alexandreas *et al.*, Paper OG 4.6.4, these proceedings; D. E. Alexandreas *et al.*, APS Proc. 1990 Meet Div. Part. Fields, Houston, Texas, Ed. B. Bonner and H. Miettinen, World Scientific, 1990.

[3] B. N. Swanenburg *et al.*, Ap. J. **243** L69 (1981).

[4] W. Forman *et al.*, Ap. J. Supp. Series **38** 357 (1978).

[5] W. Stamm and M. Samorski, in the Proceedings of 18th ICRC, Banglore, India, Vol. 1, pp.131.

[6] T. P. Li and Y. Q. Ma, Ap. J. **272** 317 (1983).

[7] M. A. Thomson *et al.*,, submitted to Phys. Lett. B.

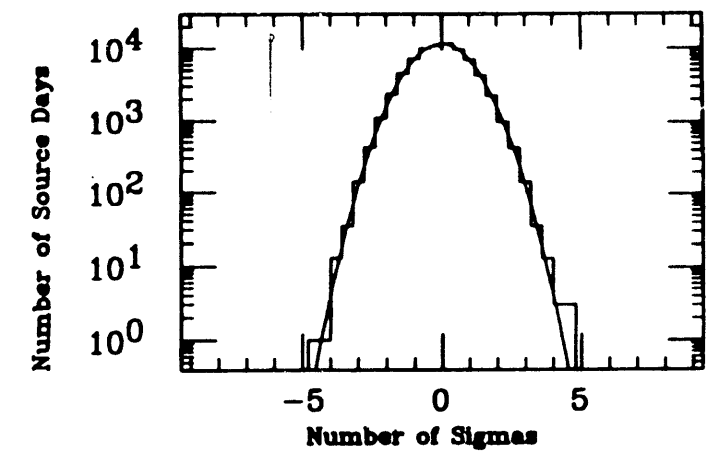

Figure 1: Distribution of daily excesses from all sources. Superimposed on the histogram is a properly normalized gaussian distribution with mean at zero and unity standard deviation. The total number of entries in the histogram is 72,865.

Table 2: List of six days that have the largest excesses.

Source	UT Date	On	Off	Excess(σ)
Crab	April 28, 1989	38	14.9	4.7
4U0352+30	Jan 17, 1990	166	117.3	4.0
4U0352+30	Aug 7, 1990	65	33.4	4.6
GK Per	Jul 23, 1987	32	12.7	4.2
HZ 43	Feb 9, 1988	46	20.2	4.6
Virgo A	Dec 2, 1989	55	27.5	4.3

Detailed Simulation of the CYGNUS Array's Response to Extensive Air Showers

The CYGNUS Collaboration

D.E. Alexandreas,[1] D. Berley,[2] S. Biller,[1] R.L. Burman,[3] D.R. Cady,[4] C.Y. Chang,[2] B.L. Dingus,[2] C. Dion,[3] G.M. Dion,[1] R.W. Ellsworth,[5] S.J. Freedman,[6] B.K. Fujikawa,[6] J.A. Goodman,[2] T.J. Haines,[3] C.M. Hoffman,[3] D.A. Krakauer,[6] P.W. Kwok,[2] X-Q Lu,[1] D.E. Nagle,[3] M. Potter,[3] V.D. Sandberg,[3] C. Sinnis,[3] M.J. Stark,[2] D. Williams,[2] G.B. Yodh,[1] and W.P. Zhang,[3]

[1] *The University of California, Irvine*
[2] *The University of Maryland, College Park*
[3] *Los Alamos National Laboratory, Los Alamos, New Mexico*
[4] *The University of Notre Dame, Notre Dame, Indiana*
[5] *George Mason University, Fairfax, Virginia*
[6] *Argonne National Laboratory*

presented by C. Sinnis

Abstract

A method for the rapid generation of simulated extensive air showers (EAS) is described. This method, consisting of SHOWERSIM (Wrotniak) combined with a library of thinned EGS4 sub-showers, follows electrons and photons down to 1 MeV; nucleons, muons and pions to below 1 GeV; and preserves the particle arrival times to 1 nanosecond. A detailed simulation of the CYGNUS detector response is also described and applied to several sets of simulated air showers.

EAS Simulation We chose the following criteria for the EAS simulation: 1) it should follow electrons, photons, muons, pions and nucleons; 2) particles should be followed until their energies fall below the minimum required to trigger each counter (~1 MeV); 3) particle arrival times should be known to ~ 1 nanosecond; 4) correlations between particle energy and arrival time should be preserved; 5) the simulation should be relatively fast (able to produce ~1000 proton showers of energy ~100 TeV in about 2 days of *real* time using a VAXSTATION 3100).

These specifications have been met by combining an updated version of SHOWERSIM (Wrotniak) with a library of lower energy, "thinned" electromagnetic sub-showers generated with EGS4 (Nelson *et. al.*).

For convenience and to preserve flexibility, the simulation of extensive air showers has been separated from that of the detector response. The air shower output is first saved as distributions that are sampled by a second simulation under various detector scenarios.

Category HE 3.6 29

Sub-Shower Library and EAS Generation The sub-shower library is composed of thinned electromagnetic showers (Hillas) initiated by electrons and photons sampled from 100 different energies (in logarithmic intervals from 5 MeV to 200 GeV); 39 initial production depths (from 0 to 800gm/cm^2 in steps of 20gm/cm^2); and 10 values of COS($\theta_{initial}$) (ranging from 1.0 to 0.17). Only those ~30000 showers with particles surviving to the CYGNUS detector level of 800gm/cm^2 are saved. These showers are stored in a direct-access file for rapid retrieval.

The appropriate sub-shower is "attached" whenever the energy of an electromagnetic particle in SHOWERSIM drops below 200 GeV . The x and y sub-shower direction cosines are then scrambled (additional randomization of the sub-shower orientation), and the sub-shower is projected onto the detector plane. For a 100 TeV proton-initiated shower, typically about one thousand these electromagnetic sub-showers are attached. Generally, one can expect to generate several hundred such proton-initiated showers in 10 real-time hours with a dedicated machine (this time is dominated by the I/O operations for accessing the sub-shower library).

Shower simulation output is taken relative to the shower plane and azimuthal symmetry about the core is assumed so that showers can be stored in terms of radius-dependent distributions. The showerfront time-structure is explicitly preserved by a 20-bin histogram of particle arrival times for each radius interval. Other distributions saved include the particle density versus radius, the average radius of particles falling in a given radial bin (for purposes of interpolation), and the average particle energy as a function of both radius and arrival time. Each of these distributions are computed and stored separately for electrons, photons, muons, nucleons and pions.

CYGNUS Detector Simulation Whenever possible, data and/or separate simulations were used to minimise arbitrary adjustments of parameters in the detector simulation. For example, the scintillator attenuation length was determined by a separate simulation of an individual counter to account for the variation in light yield due to the scintillator quality. The simulation was then compared with tests previously made with a Quanticon photomultiplier tube (PMT) that measured the number of photoelectrons detected when through-going muons pass through the scintillator. This simulation was also used to determine the distribution of arrival times as measured by the PMT relative to when a charged particle passes through the scintillator.

The number of particles striking a given counter is determined by interpolating the particle density, multiplying by the scintillator area, and then fluctuating this number according to a Poisson distribution. For each of these particles, the arrival time and energy are then sampled from the appropriate distributions.

Electron and photon energy deposition in the scintillator were modeled based on separate EGS4 simulations. For pions, a form of the distribution of energy deposition was fit to the simulation results of Ispirian, Margarian and Zverev (1974). Muons were assumed to deposit exactly the amount of energy expected for a through-going, minimum-ionizing particle (2 MeV per cm of track length).

Half of the nucleons are assumed to be high-energy neutrons that do not deposit any energy in the scintillator (n-p scattering has not been taken into account). The other half are assumed to be minimum-ionizing protons.

As in the actual experiment, the energy deposition is then defined relative to the median of the pulse height distribution obtained from single, through-going muons.

After each particle has deposited its energy in the scintillator, the number of photoelectrons generated in the PMT are calculated. This number is then fluctuated according to a Poisson distribution, and used to sample the scintillator-PMT transit time. The earliest transit time is then added to the particle arrival time and the effective particle number is re-calculated (owing to the additional fluctuation in the number of photoelectrons). Next, the ADC and TDC responses are simulated, and expected errors due to calibration uncertainties are folded in.

The entire event is then tested to determine whether the array is triggered based on criteria set up in the initial configuration. If a trigger occurs, the number of muons above detection threshold that strike the muon detector(s) is then calculated. The entire event is then written in a standard data-file format (for easy comparison with actual data), and the next event is processed.

Results As an example of the simulation's performance, a data set of "background" showers was simulated by modeling proton-initiated showers sampled from an $E^{-1.7}$ integral energy spectrum starting at 50TeV. The showers were projected from the zenith, with the core location varied over a radius of 200 meters relative to the geometric center of the array. The detector configuration simulated was that of the original 64-counter array as it existed in 1986.

The average angular resolution of triggered simulation events was ~0.65 degrees, as compared with the measured, zenith averaged value of 0.75 degrees obtained from an analysis of the sun/moon shadowing of cosmic rays (Alexandreas *et. al.*, 1991). The expected trigger rate based on simulation for various array and trigger configurations is found to be well within the bounds of uncertainties in cosmic ray flux and composition models.

Figures 1 through 3 compare simulated and measured distributions of shower sizes, the single-counter particle spectrum, and the distribution of space-angle differences obtained from fitting the same event with even and odd counters.

This work is supported in part by the National Science Foundation, Los Alamos National Laboratory, the U.S. Department of Energy, and the Institute of Geophysics and Planetary Physics of the University of California.

References

J. A. Wrotniak. *SHOWERSIM/85*. Dept. of Physics, University of Maryland

W. O. Nelson, H. Hirayama and D. W. O. Rogers. *The EGS4 Code System*. SLAC Report 265, December 1985

A. M. Hillas. Proceedings of the 17th ICRC, Paris, Vol. 8, p.193

K. A. Ispirian, A. T. Margarian and A. M. Zverev. Nuclear Instruments and Methods, 117 (1974) p. 125-129

D. E. Alexandreas *et. al.*. Phys. Rev. D., Brief Reports **43**, 1735 (1991)

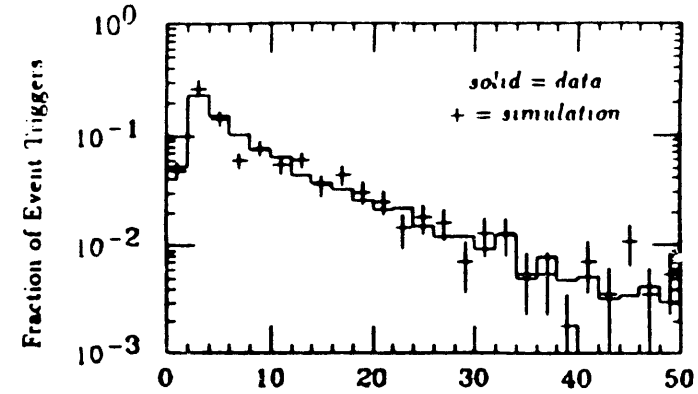

FIGURE 1 : Spectrum of Observed Shower Sizes (units of 10^4)

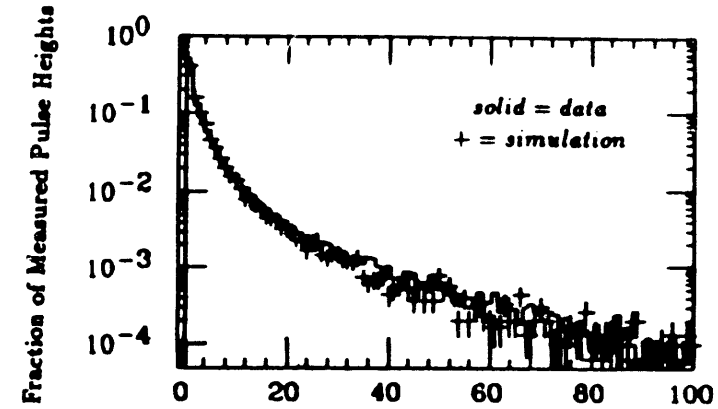

FIGURE 2 : Observed Particle Number per Detector

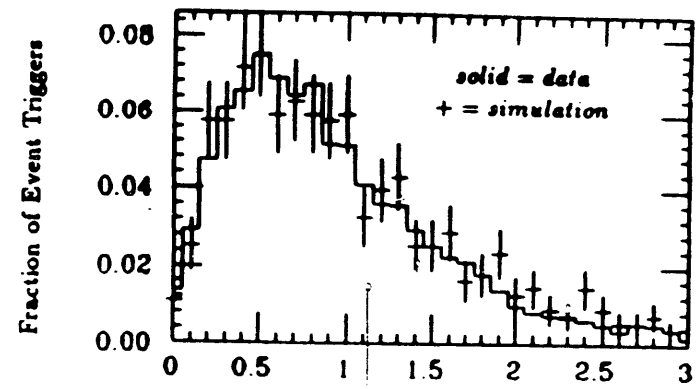

FIGURE 3 : Space-Angle Difference from Even/Odd Counter Timing Fits

Characteristics of "Anomalous Muon" Events Associated with HERCULES X-1

The CYGNUS Collaboration

D.E. Alexandreas,[1] D. Berley,[2] S. Biller,[1] R.L. Burman,[3] D.R. Cady,[4] C.Y. Chang,[2] B.L. Dingus,[2] C. Dion,[2] G.M. Dion,[1] R.W. Ellsworth,[5] S.J. Freedman,[6] B.K. Fujikawa,[6] J.A. Goodman,[2] T.J. Haines,[2] C.M. Hoffman,[3] D.A. Krakauer,[6] P.W. Kwok,[2] X-Q Lu,[1] D.E. Nagle,[3] M. Potter,[3] V.D. Sandberg,[3] C. Sinnis,[3] M.J. Stark,[2] T. Tsutsumi,[7] D. Williams,[2] D.D. Weeks,[7] G.B. Yodh,[1] and W.P. Zhang,[3]

[1] *The University of California, Irvine*
[2] *The University of Maryland, College Park*
[3] *Los Alamos National Laboratory, Los Alamos, New Mexico*
[4] *The University of Notre Dame, Notre Dame, Indiana*
[5] *George Mason University, Fairfax, Virginia*
[6] *Argonne National Laboratory*
[7] *University of New Mexico*

presented by Steven D. Biller

Abstract

The 11 events from the main phase peak of the 1986 UHE, muon-rich bursts (UT 24 July, 1986) associated with Hercules X-1 (previously reported by this group) have been studied for characteristics that might distinguish them from background showers. The most interesting effect observed results from an analysis of the showerfront thickness for these events. This analysis was then applied *a priori* to the rest of the events in the source day where, based on the observed event excess, an additional ~9 signal events are expected. The same showerfront thickness effect was observed here at a chance probability level of < 0.1% . There are also indications, though considerably less significant, of a steeper muon lateral distribution and a harder shower-size spectrum. Efforts to confirm these possible characteristics are discussed, along with attempts to link these effects to an interaction model.

Analysis of the 11 Phased, Burst Events Figure 1 shows the previously published phaseogram for the 17 events that occured during 2 episodes of particularly large rate increases (bursts "A" and "B") for the day UT 24 July, 1986 (Dingus *et. al.*). The 11 events indicated in the "main phase peak" are believed to constitue a nearly pure sample containing ~1 background event. These events were found to have an anomalously large muon content compared to that expected from gamma rays. Several other parameters have now been examined for anomalous behavior. The table below lists the "pre-trial" chance probability that the ensemble was drawn from a background distribution for various hypotheses tested. These probabilities were derived by comparison with ensembles of "similar" background events (typically chosen based on zenith angle, core location and shower size). These background events were taken from data collected within ±4 days of the original observation to insure the same detector conditions.

	Hypothesis	Chance Probability
1	Larger Shower Age	82%
2	Steeper Size Spectrum	15%
3	Larger Particle Density Fluctuations	27%
4	Larger Muon Content	5%
5	Steeper Muon Lateral Distribution	3%
6	Smaller Showerfront Curvature	33%
7	Narrower Showerfront Thickness	4%
8	Smaller Ratio of Near-Core to Peripheral Showerfront Thickness	1%

Note that the two muon analyses (4 and 5) are *not* independent, as the analysis of muon content assumes that the muon lateral distribution of the signal is like that of background. Due to the *a posteriori* nature of these various analyses, the final "post-trial" probabilities are difficult to assess. The 33 events in the rest of the source day represent an independent data set where an additional 9±5 signal events are expected from the observed event excess. For an unambiguious probability estimate, we will therefore take the analysis that yields the most significant result for the 11 events previously described, and apply it *a priori* to this independent data set. The muon lateral distribution analysis is not a candidate for this test since it can only be applied to an ensemble of events, not on an event-by-event basis (the experiment was only operating with a single muon detector at the time). The parameter chosen was the ratio of near-core to peripheral showerfront thicknesses.

This parameter is computed by first determining the detected particle arrival times relative to a curved showerfront fit. Next, for the half of the triggered counters furthest from the shower core, the width of the distribution of particle arrival times is calculated. This is also done for the counters closest to the core. The ratio of inner-counter to outer-counter timing widths is then taken to be the test parameter, hereafter refered to as W_R (width-ratio).

Analysis of the Remaining 33 Events The chance probability that the distribution of W_R in the rest of the source day was drawn from a background distribution is found to be less than 0.1% . Note that this probability is *independent* of the 11 events that were initially used to choose this parameter.

If this effect is indicative of an actual signal characteristic, then one would expect that it should manifest itself predominantly in a group of events with phases consistent with those of the previously published burst events.

A period of 1.23573 seconds was found to yield the largest value of the Protheroe statistic for the entire day, well within 1 independent Fourier spacing of the previously published period (1.23568) that was found to be optimum for the bursts alone. The 33 events from the remainder of the source day were divided into two approximately equal groups: the 16 events with the smallest W_R values; and the remaining 17 events with larger values. Figures 2 and 3 show phaseograms at this period for these two groups. The phases for the 11 previously published burst events are also shown. As can be seen, the phases of events with smaller W_R values are, indeed, more consistent with those of the 11 phased, burst events.

Discussion Since we have not yet found any other strong candidates for point-source signals in the CYGNUS data set, conclusive tests to further confirm the showerfront width hypothesis are not yet possible. However, we have looked at source days with an excess of 2σ or greater from Hercules X-1 and applied the W_R analysis with the hope of enhancing any potential weak signals. So far, all such analyses have yielded results consistent with background.

Some limited computer simulation work has been done in an attempt to link the W_R effect to the consequences of an interaction model. The results are as follows: 1) The effect is *not* reproduced by the standard interactions of protons, gammas or iron nuclei; 2) The W_R is *not* as sensitive to the depth of the primary interaction as is the shower age. This argues against a "proton-like" interaction occuring deeper in the atmosphere. Other possible mechanisms are currently being investigated.

Conclusion Detailed analysis of the events associated with the 1986 observation of Hercules X-1 indicates a difference in the structure of the showerfront thickness when compared with similar background events at a chance probability level of less than 0.1%. However, in the absence of further data capable of confirming this observation, we wish to propose this hypothesis as a highly interesting and potentially important effect in need of further study.

This work is supported in part by the National Science Foundation, Los Alamos National Laboratory, the U.S. Department of Energy, and the Institute of Geophysics and Planetary Physics of the University of California.

References

Dingus *et. al.*, 1988, Phys. Rev. Letters 61, No.17

Category OG 4.2.10

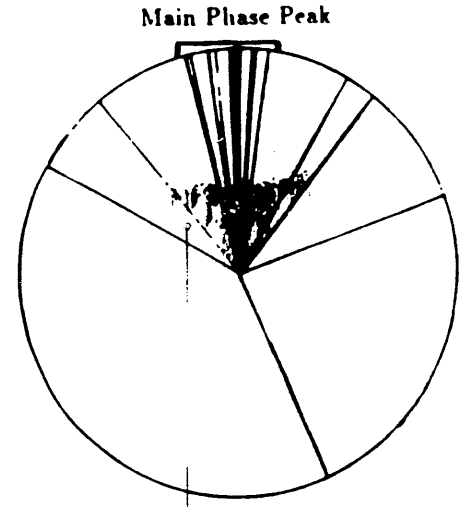

Figure 1

Previously published phaseogram of "burst" events from the 1986 observation of Hercules X-1 at the period 1.23568 seconds. This period corresponds to the most significant value of the Protheroe statistic for the 2 bursts. The 11 events occurring in the main phase peak are indicated. The origin of the phase scales for this and the following plots are arbitrary.

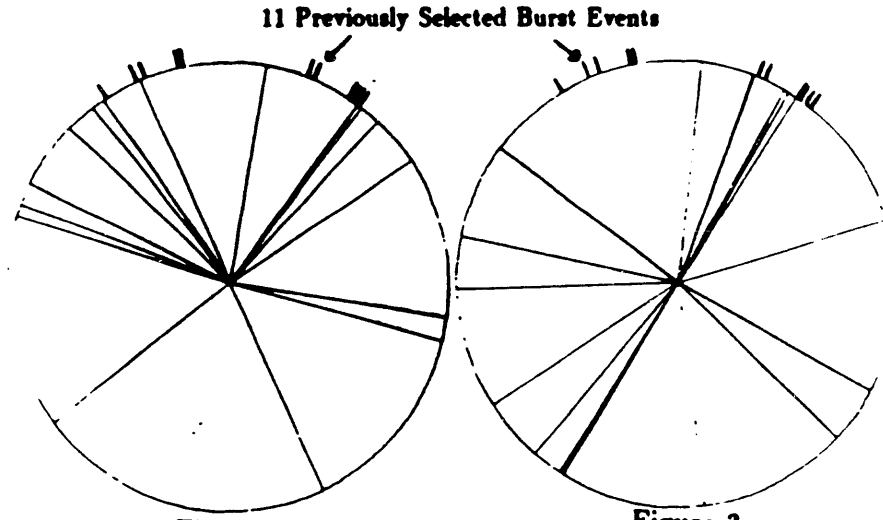

Figure 2 Figure 3

Phaseograms for the rest of the events in the source day at the period 1.23573 for events with smaller values of W_R (figure 2), and for events with larger values of W_R (figure 3). Phases for the 11 previously selected burst events are also indicated at this new period, which corresponds to the most significant value of the Protheroe statistic for the entire day.

A Search for Steady Emission from Ultra High Energy Sources

The CYGNUS Collaboration

D.E. Alexandreas,[1] D. Berley,[2] S. Biller,[1] R.L. Burman,[3] D.R. Cady,[4] C.Y. Chang,[2] B.L. Dingus,[2] C. Dion,[2] G.M. Dion,[1] R.W. Ellsworth,[5] S.J. Freedman,[6] B.K. Fujikawa,[6] J.A. Goodman,[2] T.J. Haines,[2] C.M. Hoffman,[3] D.A. Krakauer,[6] P.W. Kwok,[2] X-Q Lu,[1] D.E. Nagle,[3] M. Potter,[3] V.D. Sandberg,[3] C. Sinnis,[3] M.J. Stark,[2] T. Tsutsumi,[7] D. Williams,[2] D.D. Weeks,[7] G.B. Yodh,[1] and W.P. Zhang[3]

[1] *The University of California, Irvine, CA*
[2] *The University of Maryland, College Park, MD*
[3] *Los Alamos National Laboratory, Los Alamos, NM*
[4] *The University of Notre Dame, Notre Dame, IN*
[5] *George Mason University, Fairfax, VA*
[6] *Argonne National Laboratory, Argonne, IL*
[7] *University of New Mexico, Albuquerque, NM*

presented by Todd J. Haines

Abstract

A search has been made for steady emission of ultra high energy radiation from individual point sources over most of the northern sky. Over 200 million air showers induced by primary particles of energy greater than about 10 TeV were recorded. No statistically significant excess above the background from the isotropic flux of cosmic rays was found for any direction in the sky from 0° to 80° declination.

There have been detections reported of either steady, pulsed, or episodic emission at energies above about 1 TeV from many different sources. Only two sources, Cygnus X-3 and the Crab, have been observed as constant sources by at least two independent observations, and Cygnus X-3 apparently is no longer a source at these energies. Nevertheless, because cosmic ray particle acceleration to energies above ≈ 10 TeV is not well understood, it is important to know which astrophysical objects are potential sources at these energies; thus, the need to search for emission from a variety of previously identified lower energy sources and from undiscovered sources, i.e. an "all-sky" survey.

The CYGNUS air shower experiment operates nearly continuously and has collected about 210 million ultra high energy (UHE) air shower events during the time period between 1986 April and 1991 May. While the experiment has been described in detail elsewhere,[1] the combination of large area, low threshold, and good angular resolution make it well suited for searching for point sources of radiation at these energies.

There are many effects in an air shower experiment that, if not handled properly, could cause possible large systematic errors that could either hide a real point source or apparently create one where none actually exists. These effects include: down time, rate variations, and non-uniformities in the acceptance of the array to air showers. They can cause variations in the effective exposure of the array to different parts of the sky.

A technique has been developed[2] that is able to estimate the number of expected background events at each point in the celestial sky without having to make any cuts on the data. First, the number of observed events at each position in the sky is determined by accumulating the events in 0.2° bins in both right ascension (α) and declination (δ). Then, the background must be estimated from the data.

This is accomplished by accumulating the zenith and azimuthal angle distribution of a large number of events, $N(\theta, \phi)$. For each observed event, a random "background" event

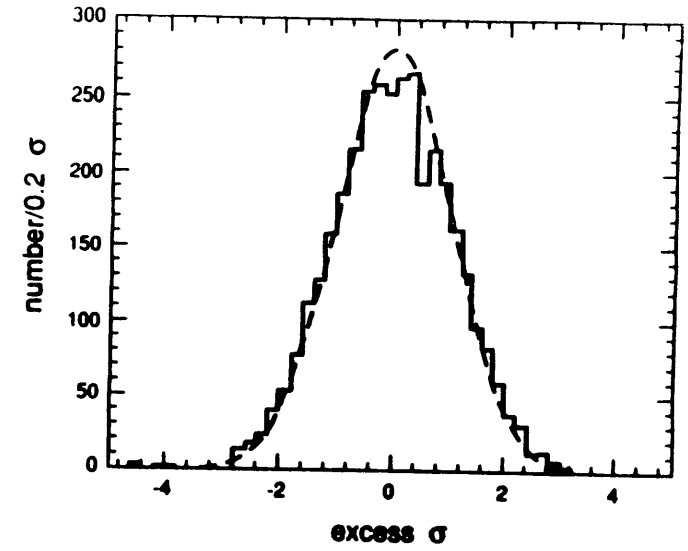

Figure 1: The distribution of the excess number of events from each of 3,600 non-overlapping bins. The dashed curve is a Gaussian distribution expected from only fluctuations of the background which fits the data well with a χ^2 of 50.8 for 49 DoF.

is created by using the event time and choosing new local coordinates randomly from $N(\theta, \phi)$; the celestial coordinates for the "background" event are then determined and binned in the same way as for the observed data. This procedure is repeated 10 times for each observed event so that the statistical uncertainty in the background estimate is relatively small. During the data processing, a new $N(\theta, \phi)$ distribution is accumulated to be used for the next set of events, thus allowing for variations in this distribution over rather short timescales. Further, because randomised events are generated using the actual event times, the method correctly accounts for periods when the experiment was not operating, as well accounting for changes in the trigger rate. Several checks have been made of the results, and no systematic errors were found.

For this analysis, a square bin is used with dimensions 2.4° in δ and 2.4°/cos(δ) in α, rounded to the nearest 0.2° in α, centered on the potential source location. For the all sky survey, the northern sky between 0° δ and 80° δ was divided into a non-overlapping grid of about 3,600 independent bins. The distribution of the excess events in each bin is shown in Figure 1. This was redone with the bins shifted by 1/2 of a bin in α, δ, and both α and δ. There is no statistically significant excess of events above background for any of the bins.

An upper limit on the flux has been calculated for each of these bins.[3] Although the minimum detectable energy for the CYGNUS array is about 10 TeV, the flux limits are given at the energy that corresponds to the peak of the observed cosmic ray spectrum, 40 TeV, by extrapolating from 10 TeV to 40 TeV according to the assumed differential spectral index γ = -2.7. Figure 2 illustrates the upper limits on the continuous flux above 40 TeV that would correspond to zero excess events for a bin, as a function of the δ of the bin.

In addition to the all sky survey, 49 potential point sources have been examined using the same method except that the bins are centered on the candidate source. The candidate

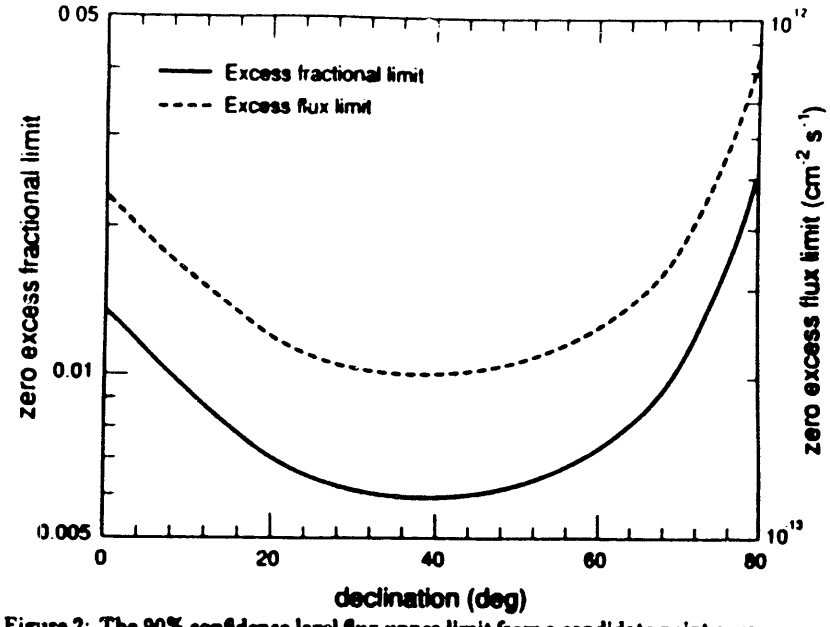

Figure 2: The 90% confidence level flux upper limit from a candidate point source assuming there is no excess events observed from the source position. The flux limits assume a differential spectral index of -2.7; the limits would be about 25% lower for a spectral index of -2.0.

source list includes previously reported very-high energy and ultra high energy sources, selected pulsars, cataclysmic variables, galaxies, and selected x-ray and γ-ray sources. No source shows a significant excess above expectation; Table 1 presents the results and flux upper limits. Some of these limits appear to be in disagreement with previously reported observations by other groups.[4]

[1] D.E. Alexandreas *et al.*, LA-UR-2167, submitted to Nucl. Inst. and Meth. in Physics Research, (June, 1991); R.C. Allen *et al.*, LA-UR-91-2142, submitted to Nucl. Inst. and Meth. in Physics Research, (June, 1991).
[2] D.E. Alexandreas *et al.*, UMD-PP-92-027, submitted to Nucl. Inst. and Meth. in Physics Research, (Aug., 1991).
[3] We have used a variant of the prescription suggested by the Particle Data Group, M. Aguilar-Benitez *et al.*, Phys. Lett. 170B, 55(1986).
[4] Y. Muraki *et al.*, Ap. J. 373, 657(1991); S.C. Tonwar *et al.*, Ap. J. 330, L107(1988).

Table 1. The limits from 49 potential point sources. N_{on} and N_{off} are the number of events observed from the source position and the number expected from the cosmic ray background, respectively, N_σ is the number of standard deviations excess above the background, F_{lim} is the 90% CL upper limit on the fractional excess above the background in percent, and F_0 is the integral flux limit above 40 TeV in units of $10^{-13} cm^{-2} s^{-1}$ assuming a differential power law spectral index of -2.7

Source	α	δ	N_{on}	N_{off}	N_σ	F_{lim}	F_0
Cyg X-3	307.7	40.8	94869	94859	0.0	0.57	1.9
Her X-1	254.0	35.4	95774	95956	-0.6	0.47	1.6
Crab	82.9	22.0	64792	64325	1.8	1.28	4.4
Cyg X-1	299.1	35.1	96308	96441	-0.4	0.48	1.6
M31	9.9	41.0	85459	85417	0.1	0.63	2.2
Virgo A	186.9	12.7	43114	42801	1.5	1.42	4.8
AM Her	273.7	49.8	86184	86688	-1.7	0.34	1.2
DQ Her	271.6	45.9	89747	90228	-1.6	0.35	1.2
U Gem	118.0	22.1	65949	66038	-0.4	0.60	2.1
SS Cygni	325.2	43.4	92466	92674	-0.4	0.51	1.7
HZ 43	198.5	29.4	85641	86178	-1.8	0.34	1.0
GK Per	52.0	43.7	84677	84351	1.1	0.90	3.0
V404 Cygni	300.4	33.8	90209	90134	0.2	0.63	2.1
Kiel 1	36.0	32.3	79694	79721	0.6	0.76	2.6
Kiel 3	270.3	42.6	93139	92784	1.2	0.85	2.0
Kiel 4	36.2	61.1	48834	49238	-1.8	0.45	1.5
Kiel 5	352.7	67.4	33514	33490	0.1	1.01	3.4
Kiel 6	3.4	25.9	71023	70593	1.6	1.15	3.9
Geminga	97.4	17.8	56673	56339	1.4	1.20	4.1
1E2259+58	344.8	58.6	57499	57718	-0.9	0.54	1.8
SS433	287.3	4.9	25457	25413	0.3	1.22	4.1
4U0042+32	10.5	32.8	80687	80683	0.7	0.79	2.7
4U0115+63	18.8	63.5	43296	43061	1.2	1.28	4.3
4U0316+41	49.1	41.4	83756	83821	-0.2	0.55	1.9
4U0352+30	58.1	30.9	79612	79366	0.9	0.85	2.9
4U0614+09	93.6	9.2	32400	32273	0.7	1.25	4.3
4U1257+28	194.4	28.2	84592	84702	0.6	0.76	2.6
4U1651+39	252.9	39.9	97619	97268	1.1	0.83	2.8
4U1837+04	279.4	5.0	25899	25831	0.4	1.28	4.3
4U1901+03	285.4	3.1	21316	21449	-0.9	0.89	3.0
4U1907+09	286.8	9.7	37507	37188	1.7	1.61	5.4
4U1918+15	289.7	15.0	50851	51124	-1.2	0.51	1.7
4U1957+40	299.3	40.5	96725	96333	1.3	0.87	3.0
4U1954+31	298.5	32.0	90849	90213	-0.6	0.48	1.6
4U2142+38	325.6	38.1	91896	90358	2.4	1.28	4.4
4U2321+58	350.3	58.6	56988	57102	-0.5	0.63	2.1
2CG065+00	290.7	28.7	87998	88075	-0.6	0.49	1.7
2CG075+00	304.8	36.4	94685	95241	-2.5	0.26	0.9
2CG078+00	305.4	39.8	96970	96795	0.6	0.69	2.3
2CG095+04	318.8	55.0	66708	67201	-1.9	0.37	1.2
2CG135+01	38.2	61.7	46889	46803	-0.6	0.67	2.3
2CG121+04	7.2	66.5	35720	35635	0.4	1.09	3.7
PSR0355+54	58.8	54.1	65304	64833	1.8	1.28	4.3
PSR0950+08	147.6	8.2	30874	31114	-1.4	0.62	2.1
PSR1929+10	292.5	10.9	40173	40301	-0.6	0.70	2.4
PSR1937+21	294.4	21.5	71285	71167	0.4	0.77	2.6
PSR1951+32	297.8	32.7	89889	90377	-1.6	0.35	1.2
PSR1953+29	298.2	29.2	88426	88620	-0.6	0.47	1.6
PSR1957+20	299.4	20.7	69072	69234	-0.6	0.53	1.8

Angular Resolution of the CYGNUS EAS Array from the Shadows of the Moon and Sun

The CYGNUS Collaboration

D.E. Alexandreas,[1] D. Berley,[2] S. Biller,[1] R.L. Burman,[3] D.R. Cady,[4] C.Y. Chang,[2] B.L. Dingus,[2] C. Dion,[2] G.M. Dion,[1] R.W. Ellsworth,[5] S.J. Freedman,[6] B.K. Fujikawa,[6] J.A. Goodman,[2] T.J. Haines,[2] C.M. Hoffman,[3] D.A. Krakauer,[6] P.W. Kwok,[2] X-Q Lu,[1] D.E. Nagle,[3] M. Potter,[3] V.D. Sandberg,[3] C. Sinnis,[3] M.J. Stark,[2] T. Tsutsumi,[7] D. Williams,[2] D.D. Weeks,[7] G.B. Yodh,[1] and W.P. Zhang,[3]

[1] *The University of California, Irvine, California 92717*
[2] *The University of Maryland, College Park, Maryland 20742*
[3] *Los Alamos National Laboratory, Los Alamos, New Mexico 87545*
[4] *The University of Notre Dame, Notre Dame, Indiana 46556*
[5] *George Mason University, Fairfax, Virginia 22030*
[6] *Argonne National Laboratory, Argonne, Illinois 60439*
[7] *University of New Mexico, Albuquerque, New Mexico 87131*

Presented by Cyrus M. Hoffman

Abstract

We report here on the continuation of a study of the shadowing of cosmic rays of energies > 30 TeV by the sun and the moon. The CYGNUS experiment has collected, as of May 1991, a total of approximately 2×10^8 reconstructed showers. The angular resolution of the array, as determined from the shape of the moon and sun shadows, has been computed with cuts on various shower properties. No statistically significant dependence is found.

Introduction: The CYGNUS collaboration operates an extensive air shower (EAS) array at Los Alamos National Laboratory (106.3°W, 35.9°N), at an altitude of 2134 m (800 g/cm^2 overburden.) The goal of the experiment is to study high energy gamma rays from point sources in the galaxy. At present, there are a total of 204 scintillation detectors distributed over an area of approximately 85,000 m^2. The experiment has been described elsewhere. [1]

The possibility of studying the shadow of high energy cosmic rays made by the moon and sun was first suggested by Clark. [2] We have reported the observation, in a data set of 1.1×10^8 showers, of the shadow of the moon and sun. [3] As of May 1991, we have increased the data set to 2.01×10^8 showers, and present here the updated results.

Analysis: The reconstructed arrival directions of showers are examined and events within 5° of the moon or sun are selected. [4] The resulting data set contains 585,523 events; the angular density of events, (number of events per square degree)

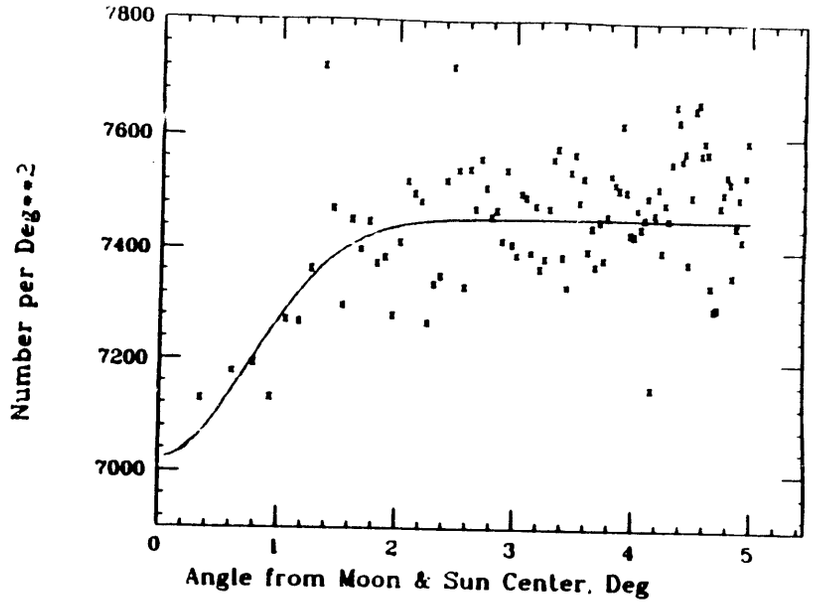

Figure 1: Angular Density, $dN/d\Omega$, of the data vs. angle from the center of the moon or sun. Solid curve is for $\sigma_r = 0.75°$.

is shown in Figure 1, where a dip near the position of the sun and moon is evident.

It is possible to verify that the depth is correct, within uncertainites, without considering its shape in detail. The measured density between 2° and 5° from the moon or sun, where shadowing is negligible, is used to calculate the expected number of events close to the sun and moon. The difference between this number and the number of observed events determines a "deficit," or number of missing events, within an angle ϑ of the center. Figure 2 shows this deficit for the combined moon and sun data. The absolute value of the total deficit can be predicted from the measured density for $\vartheta > 2°$ and the angular area of the moon and sun (6×10^{-5} sr). The measured deficit is seen to be in statistical agreement with expectations. From this graph, the statistical significance of the effect is evidently $\approx 6\sigma$. Also shown are the expected deficits for Gaussian point-spread functions.

$$P(\theta) \propto \theta e^{-\theta^2/2\sigma_r^2}$$

with standard deviations $\sigma_r = 0.50°$, $0.75°$, and $1.0°$.

Estimation of Angular Resolution: We have used the maximum likelihood method to estimate the angular resolution. We assume that the resolution function is a 2-dimensional Gaussian distribution, with a constant standard deviation, σ_r. This is used to compute the normalized probability of an event as a function of angular distance from the moon or sun center: the probability is a function of the assumed σ_r and the maximum angle in the data set. The likelihood is the

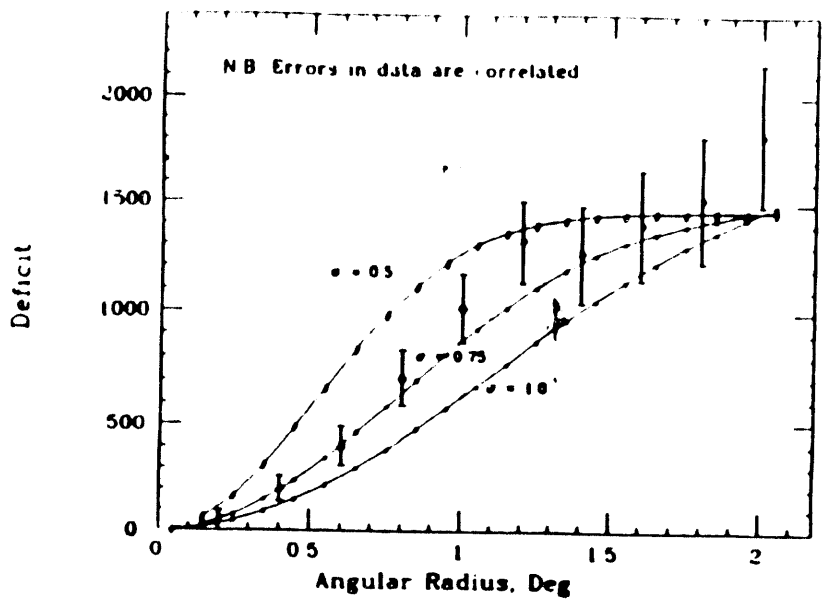

Figure 2: Deficit vs. search radius, β, for data and Gaussian densities for several values of σ_r.

product of all the probabilities, and is computed numerically for many trial σ_r's. The uncertainty in σ_r is taken to be the displacement in trial σ_r that reduces the logarithm of the likelihood by 0.5 from its maximum value. The statistical significance of the result can be estimated using the Gaussian approximation, as given by the Particle Data Group[5] for which the "number of standard deviations," N_σ is

$$N_\sigma = \sqrt{2(w_{max} - w_\infty)}$$

where w_{max} and w_∞ are the natural logarithm of the likelihood for the trial σ_r which maximises the likelihood, and for a very large σ_r, respectively. For the uncut data set, N_σ is 6.8.

Dependence on Shower Properties: We have estimated the angular resolution for subsets of the data obtained with various cuts on reconstructed shower properties. The results are shown in Table 1.

While we have expectations, based on calculations and other data analysis, of the dependence of σ_r on these shower parameters, the statistical significance obtained for the results here is not large enough to draw strong conclusions. However, dramatic dependences of the angular resolution on shower properties are excluded. For example, the difference in σ_r for showers with cores inside vs. outside the array is 1.4 σ. The 90% confidence level upper limit on σ_r for "outside" showers is 1.22°.

In the future a larger data set and improved angular resolution will allow more detailed studies of the dependence of the angular resolution on various shower properties.

Data Cuts	No. Showers	σ_r (deg)	+uncert (deg)	-uncert (deg)	N_σ
No Cuts	585,523	.75	.09	.07	6.8
Psum < 60	237,353	.74	.23	.13	3.4
60 < Psum < 150	217,985	.79	.23	.14	3.5
150 < Psum	129,329	.74	.13	.10	4.9
200 < Psum	92,850	.71	.14	.11	4.3
Zenith < 24 deg.	284,367	.75	.17	.09	4.5
Zenith > 24 deg.	301,330	.74	.12	.09	5.1
Core inside Array	398,040	.68	.08	.07	5.8
Core outside Array	186,257	.92	.23	.15	3.6

Table 1: Psum is the sum of detector signals, in numbers of effective minimum ionizing particles.

This work is supported in part by the National Science Foundation, the US Department of Energy, the Los Alamos National Laboratory, and the Institute of Geophysics and Planetary Physics of the University of California.

References

[1] Todd J. Haines et al., Arkansas Gamma-Ray and Neutrino Workshop - 1989, edited by G. B. Yodh, D. C. Wold and W. R. Kropp, Nucl. Phys. B14A 244 (1989); D. Alexandreas et al., submitted to Nuclear Instruments and Methods (1991).

[2] G. W. Clark, Phys. Rev. 108, 450 (1957).

[3] D. E. Alexandreas et al., Phys Rev D43, 1735, (1991).

[4] The moon location is obtained with a computer code based on the algorithm described in T. C. Van Flandern and K. F. Pulkkinen, Astrophysical Journal Supplement Series, 41, 391, (1979). A small (.1°- .25°) error in the code used until May 1991 has been corrected, and all events reprocessed. Parallax corrections are made to predict the α and δ of the moon as seen at the experimental site. The sun is tracked using formulae given in The Astronomical Almanac for the Year 1989, US Government Printing Office, Washington, Her Majesty's Stationery Office, London, 1989, page D3. The α and δ of each event are normally computed in epoch 1950. For comparison with data, they are precessed to the event date.

[5] Particle Data Group, Phys. Lett. B204, (1988).

Search for UHE Cosmic Rays from the Crab Nebula/Pulsar

The CYGNUS Collaboration

D.E. Alexandreas,[1] D. Berley,[2] S. Biller,[1] R.L. Burman,[3] D.R. Cady,[4] C.Y. Chang,[2] B.L. Dingus,[2] C. Dion,[2] G.M. Dion,[1] R.W. Ellsworth,[5] S.J. Freedman,[6] B.K. Fujikawa,[6] J.A. Goodman,[2] T.J. Haines,[2] C.M. Hoffman,[3] D.A. Krakauer,[6] P.W. Kwok,[2] X-Q Lu,[1] D.E. Nagle,[3] M. Potter,[3] V.D. Sandberg,[3] C. Sinnis,[3] M.J. Stark,[2] D. Williams,[2] G.B. Yodh,[1] and W.P. Zhang,[3]

[1] *The University of California, Irvine*
[2] *The University of Maryland, College Park*
[3] *Los Alamos National Laboratory, Los Alamos, New Mexico*
[4] *The University of Notre Dame, Notre Dame, Indiana*
[5] *George Mason University, Fairfax, Virginia*
[6] *Argonne National Laboratory, Argonne, Illinois*

presented by Michael J. Stark

Abstract

The CYGNUS air shower array has operated from April 1986 to the present. A search has been made for pulsed and unpulsed emission from the Crab region. We see no evidence for such emission from the Crab and set 90% confidence level upper limits on the flux from the region for steady emission at less than $6.6 \times 10^{-13}\mathrm{cm}^{-2}\mathrm{s}^{-1}$ and pulsed emission at less than $1.9 \times 10^{-13}\mathrm{cm}^{-2}\mathrm{s}^{-1}$, above 40 TeV, assuming an integral spectral index $\gamma = -1.4$

Introduction The Crab is the only known steady source of γ-rays in the 100 GeV to 4 TeV energy range.[1] VHE emission from the Crab is believed to result from inverse Compton scattering of electrons from the synchrotron-radiated photons in the nebula. This can result in an integral spectral index of $\gamma = -1.4$.[2] A cutoff in the energy spectrum is predicted in this model, but its position depends strongly on the strength of the magnetic field in the nebula; to date no cutoff has been found up to 4 TeV. Uncertainty in the cutoff energy, and the fact that the source is a close, rapidly spinning pulsar, make it an interesting source to study in UHE.

A search for emission of UHE γ-rays above ~10 TeV from the Crab using data from the CYGNUS air shower array, for the period from April 1986 through May 1991, is described here. The data set consists of 210 million air shower events: ~60,000 of these are from the Crab source bin. No evidence is found for steady, pulsed, or daily burst emission from the source and upper limits for the fluxes are obtained.

Apparatus The CYGNUS-I array began taking data in April, 1986, with 50 scintillation counters. The array was upgraded several times, described elsewhere, [3] bringing the number of CYGNUS-I counters to 108 and lowering the energy threshold; the analysis includes only a small amount of data obtained with the CYGNUS-II array. The CYGNUS-I array covers 22,000 m^2 at an atmospheric overburden of 800 gm cm^{-2}. A 44-m^2 muon detector samples the muon content of the shower.

Search for Steady Excess The method used to search for directional excess will be briefly outlined here (more details can be found in an accompanying paper).[4]

The search is made by first estimating the number of background events coming from the direction of the Crab. Detected events are characterized by the time of the event and by θ and ϕ, where θ and ϕ are the local zenith and azimuthal angles of the event direction, respectively. Ten simulated background events are then generated from each detected event time by randomly selecting θ and ϕ from the distributions in these variables obtained from the rest of the data set. This technique insures that the background events reflect the exposure and trigger conditions of the experiment as a function of time. Other methods of determining the background level agree with this method.

The θ, ϕ and event time for each background and source event are mapped into celestial coordinates, δ and α. The size of the source bin, centered on the source position, is 2.4° in δ, and 2.6° in α. The number of events in the source bin is compared with the number of background events to search for evidence of emission. The result of this analysis is that 64,792 events are observed in the Crab source bin and the expected background is 64,325. The probability of obtaining an excess of 467 events or larger from fluctuations of the background is 4% (1.75 σ). The upper limit for the flux from the source region is $6.6 \times 10^{-13}\mathrm{cm}^{-2}\mathrm{s}^{-1}$ above 40 TeV (90%CL). This result uses the measured cosmic ray flux of $2 \times 10^{-7}\mathrm{cm}^{-2}\mathrm{sr}^{-1}\mathrm{s}^{-1}$ above 10 TeV[5], and is derived with an assumed integral spectral index of $\gamma = -1.4$ for the source.

Search for Daily Excess Each source day, the time from source rising until setting, is examined for excess events from the source bin with a method similar to that described above.[6] A typical upper limit for the flux on a day in the last 1.5 years, expecting approximately 70 events for each transit of the Crab, is $1.2 \times 10^{-11}\mathrm{cm}^{-1}\mathrm{s}^{-1}$ above 40 TeV (90%CL); The day with the largest excess was UT 28 April 1989 (time of closest zenith approach at ~UTC = 22 hr), which had 38 events on source, with an expected background of 14.9 events (the experiment was only operating for part of this particular source day). The probability of observing an excess this large or larger from fluctuations of the background in the 1587 days examined is 0.2%. We do not consider this compelling evidence for emission from the Crab. The upper limit for the flux from the source on this day is $1.0 \times 10^{-10}\mathrm{cm}^{-2}\mathrm{s}^{-1}$ above 40 TeV (90%CL), assuming an integral spectral index $\gamma = -1.4$, and relative sensitivity of the detector to γ-rays over hadrons given by $R(\gamma) = 1.4$.

Other groups have reported emission from the Crab on 23 February 1989, UTC ~ 1500.[7,8,9] We have searched for possible emission from the Crab on the two days bracketing the time of the reported detection. The upper limit for the flux on the day prior to that of the claimed burst, source transit of (UTC = 2447579.5, 83600 s. to UTC = 2447580.5, 18800 s.), is $2.8 \times 10^{-11}\mathrm{cm}^{-2}\mathrm{s}^{-1}$ above 40 TeV (90%CL), and the upper limit for the flux on the day after, is $3.0 \times 10^{-11}\mathrm{cm}^{-2}\mathrm{s}^{-1}$ above 40 TeV (90%CL); in early 1989, CYGNUS was still operating at a considerably lower trigger rate than at present with only 20 events per day expected from the Crab position.

Search for Pulsed Emission The detected events from the Crab source bin have been examined for coherence with the pulsar frequency of 33 ms. The pulsar frequency and epoch are obtained from tables provided to us by Lyne and Pritchard.[10] Each entry in the table gives the period and epoch time of the main pulse at the solar system barycenter (SSBC) at monthly intervals through February 1991. Interpolation between table entries provides better than 2% accuracy in calculating the phase at any time during the month. The measured time of arrival for each event in the Crab source bin is adjusted by the propagation time from the earth to the SSBC using the JPL planetary ephemerides and

associated programs provided to us by Standish [11] The times are compared to the radio ephemeris to obtain the the pulsar phase.

Computer simulations have been made to determine the best bin size and test statistic to use for data with a mixture of background events, distributed uniformly in phase, and signal events, distributed with light curves obtained from the radio observations. For this study, the ratio of the number of source events to background events was fixed to agree with the observed excess for the source region. The signal events were distributed in phase within an envelope of single and double bump phase structures centered on the radio main and interpulse peaks of 0.0 and 0.42 respectively. Modified Rayleigh statistics, Z_n, (n=1 to n=10)[12], were tested for power as a function of bin size. The Z_8 statistic had the largest power on average; the bin size of $\Delta\delta \sim 2.4°$ optimized the power.

The phaseogram for the data, shown in Figure 1, is consistent with unpulsed background. The power for the Z_8 statistic of 3.7 is expected to be exceeded by fluctuations in the background 96% of the time. The upper limit for pulsed emission at the main phase peak is $1.6 \times 10^{-13}\mathrm{cm}^{-2}\mathrm{s}^{-1}$ above 40 TeV (90%CL). The upper limit on pulsed emission at the interpulse is $1.0 \times 10^{-13}\mathrm{cm}^{-2}\mathrm{s}^{-1}$ above 40 TeV (90%CL). The combined upper limit for the flux of $1.9 \times 10^{-13}\mathrm{cm}^{-2}\mathrm{s}^{-1}$ above 40 TeV (90%CL), when scaled up in energy to 200 TeV, is substantially lower than the flux given by the Ooty group [13], of $(4.1 \pm 1.2) \times 10^{-13}\mathrm{cm}^{-2}\mathrm{s}^{-1}$ above 200 TeV. Data from CYGNUS was obtained during a period overlapping the time of Ooty's observations, obtained in 1984-87. Events with no detected muons also show no evidence for pulsed emission from the Crab.

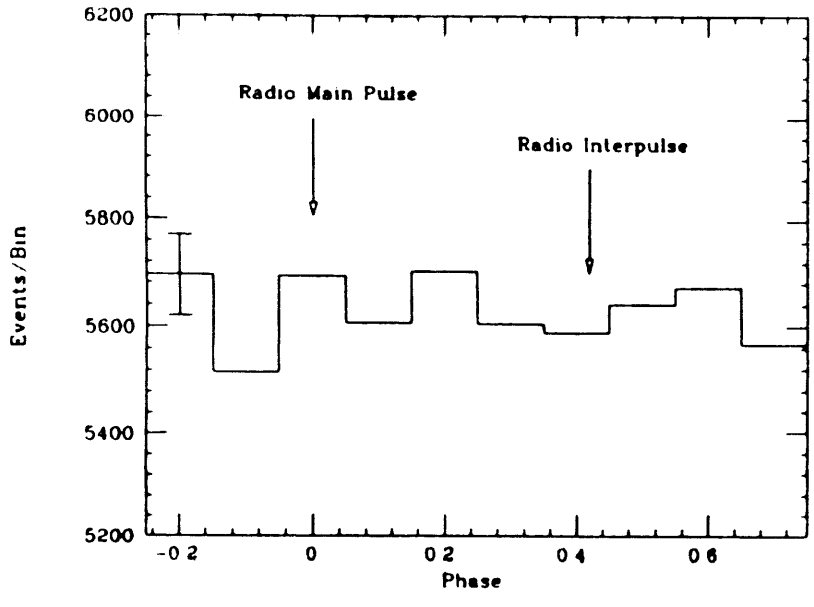

Figure 1: Crab Phaseogram, April 1986 - February 1991

Summary: We find no evidence for UHE emission from the Crab and set upper limits for the flux of steady, pulsed and burst emission for the period from April 1986 to May 1991. This period includes times in which other groups claim the observation of UHE emission from the Crab.

We would like to thank R.S. Delay for his continued efforts in maintaining the experiment as well as his contributions to recent upgrades. We would also like to thank R. Barrone, M. Gilra, E. Horch, and K. Visnovsky for their assistance in upgrades and data processing. Many of us would like to thank the MP Division of Los Alamos National Laboratory for the use of their facilities and support of this experiment. This work is supported in part by the National Science Foundation, Los Alamos National Laboratory, the U.S. Department of Energy, and the Institute of Geophysics and Planetary Physics of the University of California.

References

[1] Lamb, R.C.,*et. al.*, in *AIP Conference Proc on High Energy Gamma-Ray Astronomy*, **220**, 47, Ann Arbor, MI (1990).

[2] Gould, R.J., Phys. Rev. Lett.,**15**, 511 (1965)

[3] Alexandreas, D.E., *et. al.*, The CYGNUS Air Shower Experiment, submitted to Nuclear Instruments and Methods, June (1991).

[4] Alexandreas, D.E., *et. al.*, in these proceedings, OG 4.6.4, Dublin, Ireland (1991).

[5] Grigorov, N.L., Rapoport, I.D., Savenko, I.A., Nestorov, V.E., and Prokhin, V.L., *Proc. International Cosmic Ray Conference*,**5**,1760, Hobart, (1971)

[6] Alexandreas, D.E.,*et. al.*, in these proceedings, OG 4.3.18, Dublin, Ireland (1991).

[7] Alexeenko, V.V.,*et. al.*, *AIP Conference Proceedings, Ibid.*, **220**, 132, Ann Arbor, MI (1990).

[8] Acharya, B.S. *et. al.*, *AIP Conference Proceedings, Ibid.*, **220**, 137, Ann Arbor, MI (1990).

[9] Aglietta, M., *et. al.*, *AIP Conference Proceedings, Ibid.*, **220**, 145, Ann Arbor, MI (1990).

[10] Lyne, A.G., and Pritchard, R.S., Jodrell Bank Crab Pulsar Ephemeris Tables, unpublished (1991)

[11] Standish, M., JPL Planetary Ephemeris, magnetic tape, unpublished (1991).

[12] Nagle, D.E., Gaisser, T.K., and Protheroe, R.J., Ann. Rev. Nucl. Part. Sci., **38**, 609, (1988).

[13] Gupta, S.K., *et. al.*, Astronomy and Astrophysics, **245**, 141(1991).

SEARCH FOR PULSED UHE EMISSION FROM 4U0115+63

The CYGNUS Collaboration

D.E. Alexandreas,[1] D. Berley,[2] S. Biller,[1] R.L. Burman,[3] D.R. Cady,[4] C.Y. Chang,[2] B.L. Dingus,[2] C. Dion,[2] G.M. Dion,[1] R.W. Ellsworth,[6] S.J. Freedman,[7] B.K. Fujikawa,[7] J.A. Goodman,[2] T.J. Haines,[2] C.M. Hoffman,[3] D.A. Krakauer,[7] P.W. Kwok,[2] X-Q Lu,[1] D.E. Nagle,[3] M. Potter,[3] V.D. Sandberg,[3] C. Sinnis,[3] M.J. Stark,[2] T. Tsutsumi,[9] D. Williams,[2] D.D. Weeks,[9] G.B. Yodh,[1] and W.P. Zhang,[3]

[1] *The University of California, Irvine, California 92717*
[2] *The University of Maryland, College Park, Maryland 20742*
[3] *Los Alamos National Laboratory, Los Alamos, New Mexico 87545*
[4] *The University of Notre Dame, Notre Dame, Indiana 46556*
[6] *George Mason University, Fairfax, Virginia 22030*
[7] *Argonne National Laboratory, Argonne, Illinois 60439*
[9] *University of New Mexico, Albuquerque, New Mexico 87131*

presented by D. E. Alexandreas

Abstract

We have searched for emission from the transient X-ray pulsar 4U0115+63 in the database of the CYGNUS experiment, from April 1986 through June 1991. No significant pulsed emission is observed. A 90% confidence-level upper limit on the pulsed flux from 4U0115+63 is 4×10^{-12} cm^{-2} s^{-1} above 40 TeV.

INTRODUCTION AND OBSERVATIONS The transient X-ray pulsar 4U0115+63, first observed by the *Uhuru* satellite (Forman et al. 1976), is a neutron star with spin period 3.6 s in binary orbit with a Be companion star. The orbit has 140.1 lt-s semimajor axis, 24.3 d period and 0.34 eccentricity. The orbital parameters were first determined by Rappaport et al. 1978. The most recent ephemeris is given by Ricketts et al. 1981. 4U0115+63 has been identified with the variable discrete TeV source Cas Gamma-1 discovered by the Crimean Astrophysical Observatory (Stepanian et al. 1972, Lamb et al. 1986).

Table 1 summarizes most of the past VHE-UHE observations of the source. All detectors are Cherenkov telescopes except the last two which are air shower arrays. For positive detections, the duration of the emission is given. For the rest, the integral flux is an upper limit in units of photons cm^{-2} s^{-1}. In this last column, *d* (*p*) indicates that the flux was calculated assuming a dc (pulsed) emission. Detections have been made only by Cherenkov telescopes and only by searching for the neutron star spin period. No enhancement of the on-source counting rate over the background has ever been observed.

We report on a search in the data base of the CYGNUS experiment (April 1986 - June 1991) for pulsed emission from 4U0115+63. CYGNUS consists of an extensive air shower array and muon detectors located in Los Alamos, NM, where

Group	Observation	Threshold	Duration	Integral Flux
Crimea [17]	'71 - '73	2 TeV	two months	$3.0\ 10^{-10}$, d
Dugway [9]	Sep '84	1 TeV	continuous	$7.0\ 10^{-11}$, p
Whipple [12]	'85 - '88	0.7 TeV		$< 1.0\ 10^{-11}$, p
Pachmarhi[7]	Winter '86	1.5 TeV	2-3 hrs	$2.7\ 10^{-11}$, p
Gulmarg [14]	'87 - '88	2 TeV	1950 s	$1.8\ 10^{-10}$, p
Pachmarhi[1]	Oct - Nov '87	1.5 TeV		$< 6.0\ 10^{-12}$, p
La Palma [8]	Sep - Oct '88	0.4 TeV	continuous	$4.4\ 10^{-10}$, p
Plateau Rosa[13]	Feb '82 - Dec '87	30 TeV		$< 4.1\ 10^{-12}$, d
EAS Top [2]	'88 - '89	150 TeV		$< 1.9\ 10^{-13}$, d

Table 1: Summary of past observations.

the atmospheric overburden is 800 g cm^{-2} (Alexandreas et al. 1991). The 204 scintillation counters cover 85,000 m^2. The uncertainty in the arrival direction of air-showers is 0.75°. Most of the data analyzed here is from the CYG I array that had 108 counters covering 25,000 m^2.

SEARCH FOR PULSED EMISSION We apply here the same method of analysis used by Macomb et al. 1991 for the Whipple observatory data. We use two search ranges around the X-ray period of 3.6146643 s: (1) a wide one (3.60386 s - 3.62546 s) to accomodate period shifts like those observed between TeV and X-ray observations of Hercules X-1, and (2) a narrow one (3.61356 s - 3.61576 s) for the observed X-ray period derivatives. The data consist of the arrival times (reduced to the solar system and the binary orbit barycenters) of the air showers recorded in a 4.1° × 9.2° bin centered on 4U0115+63, chosen to include 90% of the signal from a point source. Among the 1677 days (segments) when the source passed overhead, the shortest segment lasted 1.7 hr and the longest 13 hr. This implies a maximum independent period spacing of 2.2 ms and a minimum of 0.28 ms. We scan each period range in steps of 0.05 ms, resulting in an oversampling of at least 5. We analyze each segment separately: from the arrival times in each day, we calculate the Rayleigh power, z, for each of the 433 (45) periods in the wide (narrow) search range and the probability P(> z) of observing a power larger than z. The formula for this probability is valid only for segments with at least 14 events, thus reducing the data set to 1473 days. For the background, we scan a period range that is next to the wide one mentioned above and is five times wider.

To search for bursts, we examine the data for the presense of anomalously high powers: the number of times that we got a power greater than z in all the days and periods scanned is plotted in Figure 1 against P(> z). No deviations from the background are seen.

Next we examine the possibility of continuous pulsed emission, as in the detection by Chadwick et al. 1985. A sensitive test is the incoherent sum of the Rayleigh powers. In the absence of a signal, twice the power is distributed as χ^2 with number of degrees of freedom equal to twice the number of segments. Figure 2 shows the frequency spectrum that results from such an incoherent sum for the source and background searches; the ordinate is the total power divided by

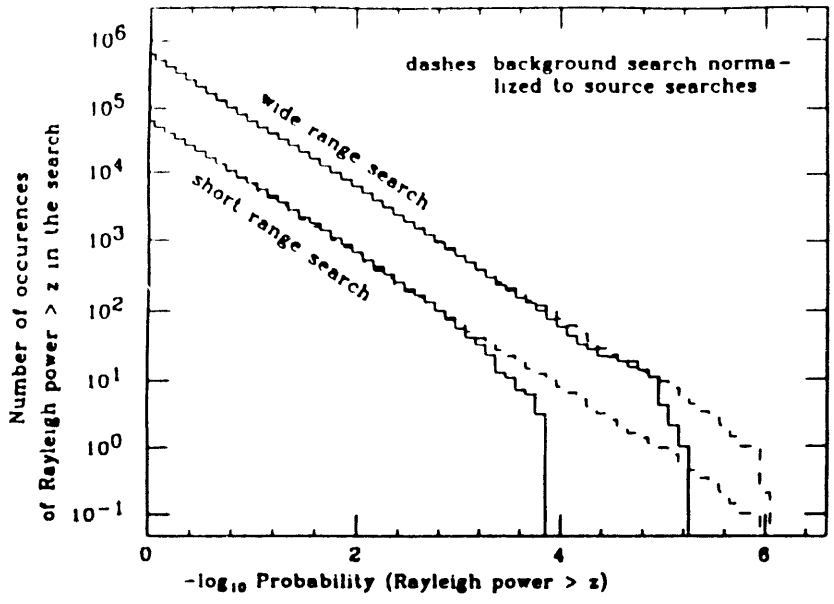

Figure 1: Cumulative probability distribution of the daily Rayleigh powers.

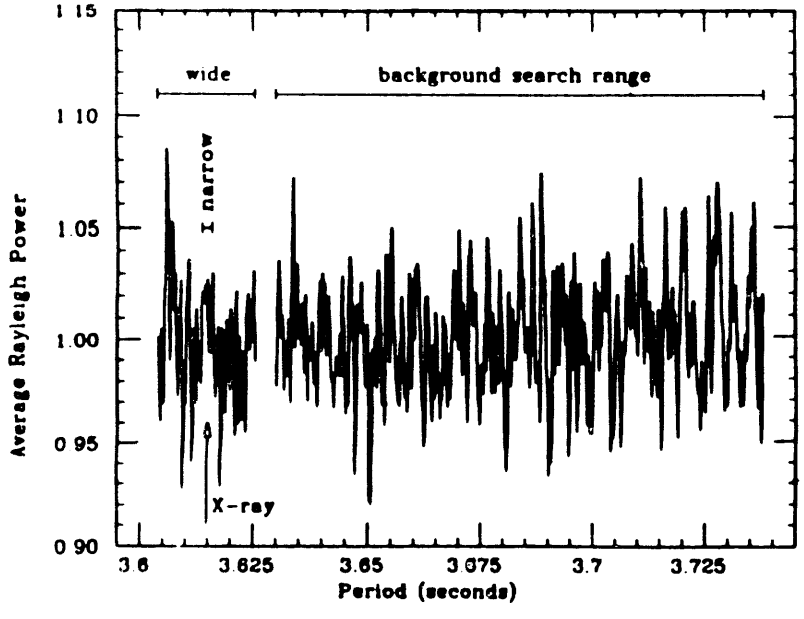

Figure 2: Frequency spectrum of the incoherent sum of Rayleigh powers. The ordinate is the total power divided by the total number of days.

the number of segments. The highest average power in the wide (narrow) search range is 1.085 (1.027) with probability of 0.0007 (0.15). There are between 10 and 100 independent periods in the wide range search and another trials factor of 3 for oversampling. We will investigate further this 0.0007 probability. We assume a sinusoidal light curve (Chadwick et al. 1985, Whitlock et al. 1989). On the average there are 89 events in a segment. Then the maximum incoherent powers mentioned above imply a 90% confidence-level upper limit for the flux in the case of steady pulsed emission from 4U0115+63 of 4×10^{-12} cm^{-2} s^{-1} above 40 TeV.

We report elsewhere on a search for dc emission from 4U0115+63 and other sources (Alexandreas et al. 1991a, 1991b). A 90% confidence-level upper limit on the dc flux from 4U0115+63 is 4.3×10^{-13} cm^{-2} s^{-1} above 40 TeV. Last year we also reported that a search for dc emission on a day-to-day basis did not reveal any bursts for the source, and that no correlation of emission with the orbital period was observed (Alexandreas et al. 1990). These conclusions still apply in the enlarged data set that extends through June 1991.

ACKNOWLEDGEMENTS We would like to thank R. C. Lamb for the binary orbit barycentering routine. Many of us would like to thank the MP Division of the Los Alamos National Laboratory for their kind hospitality. We would also like to thank R. Scott Delay for his efforts in keeping the experiment operating. This work was supported in part by the National Science Foundation, the U.S. Department of Energy, and the Institute of Geophysics and Planetary Physics of the University of California.

REFERENCES

[1] Acharya, B. S., et al. 1990, *XXI ICRC Adelaide Proc.*, 2, OG 4.6-5, 319.
[2] Aglietta, M., et al. 1990, *XXI ICRC Adelaide Proc.*, 2, OG 4.6-17, 345.
[3] Alexandreas, D. E., et al. 1990, *High Energy Gamma-Ray Astronomy, editor J. Matthews*, 167.
[4] Alexandreas, D. E., et al. 1991; submitted to *Nuclear Instr. and Methods.*
[5] Alexandreas, D. E., et al. 1991a, submitted to *Ap. J. (Letters).*
[6] Alexandreas, D. E., et al. 1991b, these proceedings, OG 4.6-4.
[7] Bhat, P. N., et al. 1987, (see R. J. Protheroe, XX ICRC Moscow Proc.) 8, 36.
[8] Brazier, K. T. S., et al. 1990, *XXI ICRC Adelaide Proc.*, 2, OG 4.6-29, 379.
[9] Chadwick, P. M., et al. 1985, *Astron. Astrophys.*, 151, L1.
[10] Forman, W., Jones, C., and Tananbaum, H. 1976, *Ap. J. (Letters)*, 206, L29.
[11] Lamb, R. C., and Weeks, T. C. 1988, *Astrophys. Lett.*, 25, 73.
[12] Macomb, D. J., et al., to appear in *Ap. J.*, Aug. 1, 1991.
[13] Morello, C., et al. 1990, *XXI ICRC Adelaide Proc.*, 2, OG 4.6-18, 349.
[14] Rannot, R. C., et al. 1990, *XXI ICRC Adelaide Proc.*, 2, OG 4.6-4, 315.
[15] Rappaport, S., et al. 1978, *Ap. J. (Letters)*, 224, L1.
[16] Ricketts, M. J., et al. 1981, *Space Science Reviews*, 30, 399.
[17] Stepanian, A. A., et al., *Nature Phys. Sci.*, 239, 40.
[18] Whitlock, L., et al. 1989, *Ap. J.*, 338, 381.

JASA: Initial Results from a Prototype Water-Čerenkov Air-Shower Detector

The JASA Collaboration
D. Berley, C.L. Dion, J.A. Goodman, T.J. Haines, P.W. Kwok, M.J. Stark
The University of Maryland, College Park, MD
R.C. Svoboda
Louisiana State University, Baton Rouge, LA
H. Razani
Royal Institute of Technology, Stockholm, Sweden
H. Ferguson, C.M. Hoffman, E. Horch, C. Sinnis
Los Alamos National Laboratory, Los Alamos, NM
R.W. Ellsworth
George Mason University, Fairfax, VA
R.S. Delay, X-Q. Lu, G.B. Yodh
The University of California, Irvine, CA

presented by Jordan A. Goodman

Abstract

A pilot experiment to examine the use of the water-Čerenkov technique for air shower detection was installed near the center of the CYGNUS air shower array. Preliminary results on its response to air showers, that are in general agreement with expectations, are presented. The improvements provided by the water-Čerenkov technique promise to offer significant advances for VHE-UHE γ-ray astronomy.

An air shower array may be improved most rapidly for point source sensitivity by either lowering the energy threshold or improving the angular resolution, or both. An obvious way to lower an array's threshold is to simply pack scintillation detectors close together; this has been examined[1] and shown not to be a viable alternative because the resulting angular resolution is not very good and the cost of the array is high.

During the last decade, the water-Čerenkov technique has proven to be a cost effective method for large, fully sensitive particle detectors. It is in providing the potential improvement in both threshold and angular resolution that the water-Čerenkov technique holds most promise as a next generation air-shower detector. The reason for the improvement is that a water-Čerenkov detector is sensitive over its entire surface to all components of the air shower: the electronic, photonic, muonic, and hadronic components will all be observed.

A pilot water-Čerenkov experiment was built to verify the simulations of such a detector's response. The advantage of performing the pilot experiment in coincidence with an existing air shower array is that the air shower array can determine many of the characteristics of each shower that the water detector observes: the direction, shower size, and core location can all be determined by the air shower array with sufficient accuracy.

Such a pilot experiment, named JASA, was run near the center of the CYGNUS air shower array in Los Alamos, NM at an altitude of 2,100 m. Details of the CYGNUS experiment can be found elsewhere[2] along with more details about JASA.[3] The pilot experiment is located within the CYG-I array, shown in Figure 1; this part of the array is the most densely covered with 108 detectors, separated by 15 m. Each detector is about 1 m^2 of scintillator viewed by a single phototube. The angular resolution of the CYGNUS array is about 0.75°, the typical energy of a cosmic ray is about 40 TeV, and the trigger rate is currently about 5 events per second.

A backyard-style swimming pool of radius 3.7 m (42 m^2 area) provides the water enclosure for the pilot experiment; a light-tight black PVC cover and black plastic lining

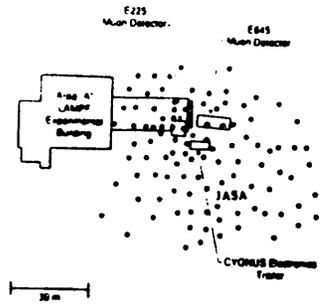

Figure 1: Deployment of counters in CYG-I; each point represents a counter. Also shown is the location of the water-Čerenkov detector.

assure minimal light reflection from the inner surfaces of the pool. The total depth of the pool, about 2.3 m, provides $\sim$ 2 m of water above the faces of the photomultiplier tubes (PMTs). There were eight 8" Hamamatsu PMTs located near the center of the pool and 2 additional 10" Burle PMTs, with much better timing characteristics (jitter < 2.5 ns FWHM), placed in the pool to improve the timing measurements.

The pool was run in coincidence with the CYG-I air shower array; preliminary results on air-shower timing measurements from these data will be given here with more refined results still to be completed.

The angular resolution of a water-Čerenkov air-shower array, like conventional arrays, depends critically on the timing of the air shower front and the timing ability of the PMTs; unlike conventional arrays, it also depends on the particular geometry of the Čerenkov light pattern which depends, in turn, on the energies and directions of the shower particles.

The timing response of the PMTs in the pool was measured by using the results of the fit to the shower plane from the CYGNUS scintillator data. Briefly, the scintillator times were first corrected for shower front curvature and then fit to a plane shower front. The plane fit is then used to predict the time that each PMT in the pool is expected to register; this time is compared with the actual time the PMT registered to determine the timing response of the water-Čerenkov detector relative to the shower plane. Both core-distance-dependent ("curvature") and pulse-height-dependent ("sampling") corrections to the PMT data are necessary. Additionally, PMT signals > 9 ns from the expected time or with pulses smaller than 3 photoelectrons (pes) are cut to eliminate the relatively long tail of small, late hits. Figure 2 shows the average time of the signals from the PMTs relative to the air shower plane for core distances between 20 and 30 m; superimposed on this figure is a Gaussian distribution with width 1.9 ns, which gives a relatively good fit to the data.

The angular resolution of the CYGNUS array ultimately limits the ability to predict the time the air shower reaches the pool and thus limits the measurement of the relative time with respect to the air shower front. Table 1 gives the rms of a Gaussian distribution fit to the relative time of the signal from the PMTs, along with the contribution of the uncertainty of the air shower direction to the timing uncertainty ($\sigma_{EAS}(ns) = 0.04 \times R_{core}(m)$). It is apparent that there is little dependence of the width of the water-Čerenkov detector timing on core distance after the contribution of the uncertainty in air shower direction is subtracted. This is also verified by noting that the rms deviation of the time of the signals from the PMTs about their mean time, used as a measure of the timing uncertainty of the pool alone, changes only slightly with core distance.

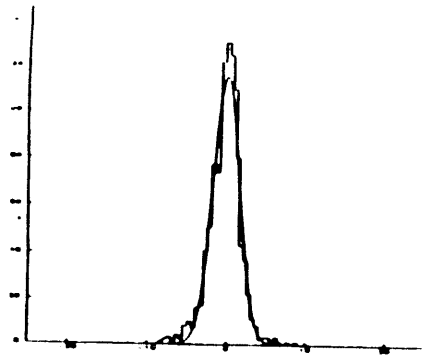

Figure 2: Average time of the PMTs relative to the air shower front.

Core Dist. (m)	σ_{PMTs} (ns)	σ_{Bur} (ns)	σ_{EAS} (ns)	RMS (ns)
0 - 10	1.45	1.75	0.2	2.17
10 - 20	1.60	1.80	0.6	2.06
20 - 30	1.80	2.03	1.0	2.20
30 - 50	2.20	2.35	1.6	2.31
50 - 75	2.95	2.80	2.5	2.44

Table 1: The timing width (σ_{PMTs}) of all PMTs in the pool ($\pm \sim 0.1$ ns). σ_{Bur} is the timing width of the Burle PMTs, σ_{EAS} is the uncertainty in EAS direction, and RMS is the rms deviation of the PMTs about their mean time.

The pulse height distribution of the signals from the PMTs will depend not simply on the number of particles hitting the pool, but also their energy and position. For example, a single through-going muon is expected to deposit an average of $\sim$ 100 pes in the pool, but the number varies greatly depending on whether the muon passes near a PMT in the center of the pool or passes just inside the edge of the pool. Nevertheless, the total pulse height of the PMT signals should depend roughly on the number of particles (N_e) hitting the pool; it is only a rough dependence since the pool is recording Čerenkov light from photons and muons in the air shower, not just from electrons, and the energy of the (electromagnetic) particles depends on the distance from the shower core.

For each air shower, the number of particles hitting the pool is derived from an NKG fit to the lateral distribution of pulse heights recorded in the CYGNUS scintillator counters. The dependence of the amount of recorded Čerenkov light on the number of particles striking the pool is shown in Figure 3. Notice in this figure that, for small particle density (around a density of 0.1 m^{-2}), the distribution divides into two with most of the events following a rough $N_{pe} \propto N_e$ relation and the rest having a substantially larger amount of recorded Čerenkov light. These latter events are apparently due to muons in the pool, perhaps showing such a pool is useful also as a surface muon detector, but before a conclusion can be reached further study is warranted.

The results are encouraging. Several additional pools are being deployed around the edges of the CYG-I array. The goal is to continue the effort at understanding the response

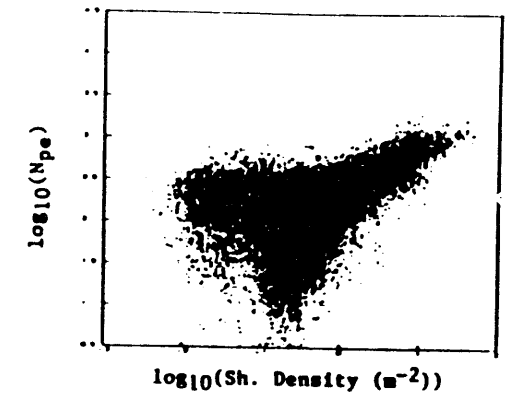

Figure 3: The total amount of Čerenkov light recorded in the pool (N_{pe}) as a function of the particle (N_e) density at the pool location, derived from a fit to the shower. The pool has a total surface area of about 42 m^2.

of a water-Čerenkov air shower detector, allowing more detailed studies of the timing and pulse height response; the additional pools should also improve the angular resolution of the CYGNUS experiment to about 0.5°.[4]

Though more detailed studies must be done, the performance of the pilot experiment is in rather good agreement with the expectations based on Monte Carlo simulations of the air shower and the response of the detector to the air showers. This lends important experimental support to the idea that large area air shower arrays based on the water-Čerenkov technique hold great promise in advancing the field of VHE-UHE γ-ray astronomy into the future.

We would like to thank the IMB collaboration and MP Division of LANL for lending us the PMTs used in this experiment, and our many hard working colleagues in the CYGNUS collaboration. This work was supported in part by the National Science Foundation, the U.S. Department of Energy, and the Los Alamos National Laboratory.

References

[1] T.J. Haines *et al.*, Proc. of the Workshop on the Physics an Experimental Techniques of High-Energy Neutrino and VHE and UHE Gamma-Ray Particle Astrophysics, G. Yodh, D. Wold, and W. Kropp, eds., Nucl. Phys. B-Proc. Supp. 14A, 244(1989).

[2] D.E. Alexandreas *et al.*, submitted to Nucl. Inst. and Methods in Physics Research, (1991).

[3] D. Berley *et al.*, Proc. of the Workshop on High Energy Gamma-Ray Astronomy, AIP Conf. Proc. 220, J. Matthews, ed., 310(1990).

[4] D.E. Alexandreas *et al.*, OG 10.4.5, these proceedings.

Studies on Improving the Angular Resolution of the CYGNUS Array

The CYGNUS Collaboration

D.E. Alexandreas,[1] D. Berley,[2] S. Biller,[1] R.L. Burman,[3] D.R. Cady,[4] M. Cavalli-Sforza,[5] C.Y. Chang,[2] D.G. Coyne,[6] B.L. Dingus,[2] C.L. Dion,[2] G.M. Dion,[1] D.E. Dorfan,[5] R.W. Ellsworth,[5] S.J. Freedman,[6] B.K. Fujikawa,[6] J.A. Goodman,[2] T.J. Haines,[2] C.M. Hoffman,[3] D.A. Krakauer,[6] P.W. Kwok,[2] X-Q Lu,[1] D.E. Nagle,[3] M. Potter,[3] V.D. Sandberg,[3] C. Sinnis,[3] M.J. Stark,[2] T. Tsutsumi,[7] D.A. Williams,[8] D.H. Williams,[2] D.D. Weeks,[7] G.B. Yodh,[1] and W.P. Zhang,[3]

[1] *The University of California, Irvine*
[2] *The University of Maryland, College Park*
[3] *Los Alamos National Laboratory, Los Alamos, New Mexico*
[4] *The University of Notre Dame, Notre Dame, Indiana*
[5] *George Mason University, Fairfax, Virginia*
[6] *Argonne National Laboratory, Argonne, Illinois*
[7] *The University of New Mexico, Albuquerque, New Mexico*
[8] *The University of California, Santa Cruz*

presented by Cynthia L. Dion

Abstract

The CYGNUS collaboration is constructing five large water Čerenkov detectors (pools), within the CYGNUS I scintillator array to improve the array's angular resolution. Monte Carlo simulations of the pools' response to extensive air showers are described.

Introduction A straightforward method of improving the angular resolution of an extensive air shower array is to increase the sampling of the particle arrival time distribution far from the core. The distribution of particle arrival times is rather wide far from the core, and has a large non-Gaussian tail of late particles. However sampling many times from this distribution and keeping only the earliest time, results in a nearly Gaussian distribution that is significantly narrower than the parent distribution. Since particle density decreases rapidly as the distance from the core increases a large area detector that is also sensitive to the photon component of air showers is desirable.

The CYGNUS collaboration has undertaken the construction of five 16,000 *gal* water Čerenkov detectors, each instrumented with seven photomultiplier tubes. In this paper we discuss the response of these pools to air showers. We pay particular attention to how the spacing and depth of the pools affects the angular resolution.

Monte Carlo Simulation of Pools Showersim (Wrotniak 1985) in conjuction with a library of EGS4 subshowers is used generate extensive air showers (Alexandreas, *et al.* 1991a). The resulting particle densities (averaged over azimuthal angle), along with energy and arrival time distributions are stored in histogram form.

Since particle densities and energies change rapidly near the core, each pool is segmented into ten regions along a line connecting the shower core to the center of the pool. For each region the density of electrons, photons, and muons is found, and multiplied by the area of each region. This number is fluctuated according to a Poisson distribution to find the number of incident particles of each type. The energy and arrival time distributions are then sampled to find the energy and arrival time of each incident particle.

The positions and azimuthal angles of the incident particles are thrown randomly, while the angle from the incident shower direction is drawn from an energy-dependent distribution (peaking along the direction of the primary). Incident photons are converted to electrons by Compton scattering and pair production. Charged particles suffer only ionization losses (multiple scattering is ignored). The Čerenkov photon density and arrival time at each PMT is found from the geometry of the incident particle's trajectory. The photon density is multiplied by the quantum efficiency of the PMTs and the overlap area between the photocathode and the Čerenkov cone. This number is fluctuated according to a Poisson distribution to find the number of detected photoelectrons in each PMT.

Investigation of Pool Spacing and Depth For a fixed number of detectors the angular resolution of an array is proportional to σ_t/R, where σ_t is the uncertainty in the measured arrival time (due to shower front width and electronic response) and R is the distance between detectors. For each radius we find the rms of the time distribution, add this in quadrature with an 1 *ns* electronic jitter, and divide by the distance from the core. The results are shown as the dashed curve in Figure 1. The solid curve corresponds to electronics with no jitter. The minimum of the dashed curve is at a core distance of $\sim 60\ m$. Because the particle density decreases with increasing distance from the core, the optimal pool spacing is somewhat less than 60 *m*.

The depth of each pool should be chosen to maximize the ratio of detected to incident particles, while keeping to a minimum the probability that the Čerenkov light from an incident particle will fall on more the one PMT. We have run the simulation for an 8 *m* diameter pool with depths of 1 *m* and 2 *m*. Six of the PMTs are arranged in hexagon 2 *m* from the pool's center, and the seventh PMT is located at the center of the pool. For a pool depth of 2 *m* there is a 25% probability of detecting an incident particle, while for depth of 1 *m* the detection probability is 10%. Based on the above results the pools will be 2 *m* deep and arranged in a rough cross pattern with $\sim 60\ m$ arms (Figure 2).

The Angular Resolution of the Pools Sixty thousand proton showers were generated according to an $E^{-2.7}$ differential spectrum, over 283,000 m^2 centered on the CYGNUS I array. These showers are passed through a simulation of the scintillator array (Alexandreas, *et al.* 1991a) and if the array generates a trigger the pool simulation is called) (roughly 1000 of the showers triggered the array; the pool information is not used in the trigger.

In Figure 3 we show the resulting, curvature corrected, arrival time distribution. To find the angular resolution of the pools we use the scintillator array to locate the core of each shower and the pool times and positions to reconstruct the primary direction. We demand that at least four pools have more than 10 photoelectrons before reconstructing the direction of the primary. With this requirement we are able to reconstruct roughly 70% of all showers which trigger the scintillator array. The resulting distribution of space angle differences between the actual and reconstructed direction is shown as the solid curve in Figure 4.

For comparison we have plotted the same distribution when only scintillator information is used to reconstruct the primary direction. The pool distribution (solid line) corresponds to an angular resolution of 0.50°, whereas the dashed distribution implies an angular resolution of 0.75° (the measured angular resolution of the CYGNUS scintillator array is 0.75° (Alexandreas *et al.* 1991b)).

Conclusions Based on the above simulation results and data taken with a prototype pool (Alexandreas, *et al.* 1991c), the collaboration has begun the construction of four more pools. It is hoped that with a careful study of curvature and sampling corrections, and by using both pool and scintillator information, we can make further improvements in the angular resolution. We are currently instrumenting the pools with PMTs and they will be placed in the data stream within two months.

References

Alexandreas, D.E.,*et al.*, 1991a, these proceedings, HE 3.6.29
Alexandreas, D.E.,*et al.*, 1991b, these proceedings, OG 10.4.4
Berley, D. *et al.*, 1991c, these proceedings, OG 10.4.6
Wrotniak, J.A., 1985, *SHOWERSIM/84*, University of Maryland Report PP85-191

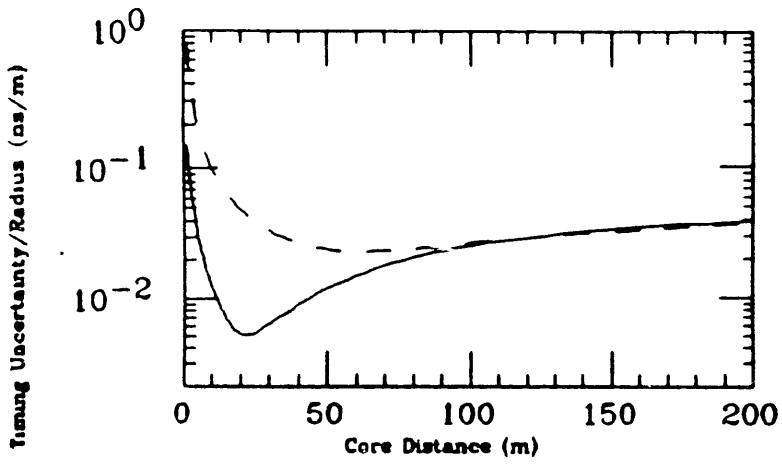

Figure 1: Uncertainty in shower front arrival time divided by the distance from the shower core versus the distance from the shower core. The solid line corresponds to no electronic uncertainty and the dashed line to an electronic uncertainty of 1 *ns*.

OG 10.4.5

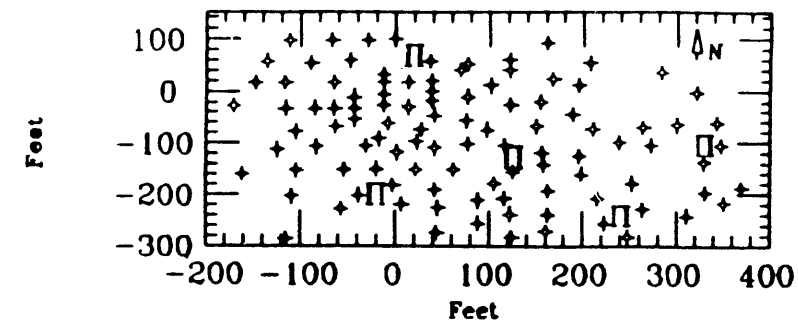

Figure 2: Layout of CYGNUS I scintillator array and 5 water Čerenkov detectors. The Π 's represent the pools, while the stars are scintillators.

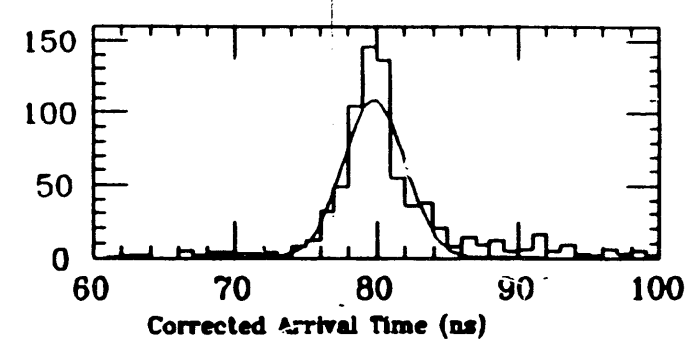

Figure 3: Predicted arrival time distribution in pools. The curve is a fitted Gaussian with a width of 2.2 *ns*

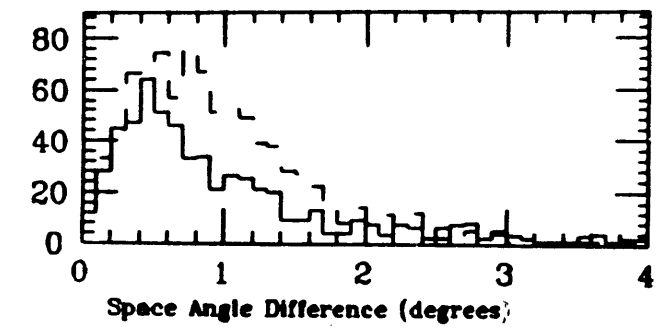

Figure 4: Distribution of space angle differences between the direction of the primary particle. Dashed line is using only the scintillator array. Solid line using only pool information.

END

DATE FILMED

10 / 22 / 91